Published Online First: July, 2024
https://doi.org/10.21123/bsj.2024.9346
P-ISSN: 2078-8665 - E-ISSN: 2411-7986
Baghdad Science Journal

Characterization of the Green Fabrication of Silver Nanoparticles by Orange Peel Extract and Their Impact on the Degradation of Halocarbon Chemical Compounds

Hisham Rasheed Rahman [1], ***Heman Burhanalden Abdulrahman*** [2], ***Rosure Borhanalden Abdulrahman**** [1]

[1]Department of Physics, College of Science, University of Kirkuk, Kirkuk, Iraq.
[2]Department of Pharmacology and Toxicology, College of Pharmacy, University of Kirkuk, Kirkuk, Iraq.
*Corresponding Author.

Received 10/09/2023, Revised 18/12/2023, Accepted 20/12/2023, Published Online First 20/07/2024

Abstract

The role of nanotechnology in remediating organic pollutants is substantial, considering the significant environmental consequences arising from the extensive agricultural use of pesticides. Consequently, nano adsorbents have attracted particular attention due to their exceptional properties and capacity to effectively degrade and eliminate various organic pollutants, including pesticides. Here, an attempt was made to fabricate and characterize silver nanoparticles (Ag NPs) using orange peel extract as a reducing agent. Transmission Electron Microscopy (TEM) images confirm the quasi-spherical shape of the Ag NPs, with average sizes of 40 nm, 30 nm, and 20 nm corresponding to different silver nitrate concentrations (0.5, 1, and 2 moles). UV-VIS Spectroscopy analysis revealed absorption peaks at 427 nm, 429 nm, and 437 nm for sizes of 20 nm, 30 nm, and 40 nm, respectively, highlighting the correlation between size and optical characteristics reveals that there is a noticeable redshift in absorption peaks as size increases. Zeta potential analysis indicated moderate stability for the fabricated nanoparticles, with values of -26.6 mV, -25 mV, and -24 mV for nanoparticles of sizes 20 nm, 30 nm, and 40 nm, respectively. X-ray diffraction (XRD) analysis confirmed the presence of a polycrystalline structure with a cubic crystal phase of fabricated Ag NPs with crystallite sizes of approximately 11.0839 nm, 11.0694 nm, and 10.2993 nm for 20 nm, 30 nm, and 40 nm nanoparticles, respectively. Fourier-transform infrared (FTIR) analysis exhibited functional groups from the orange peel extract on the nanoparticles' surfaces, enhancing their stability and bioactivity. Additionally, the interaction between Ag NPs and three different pesticides (Cypermethrin, Lambda-cyhalothrin, and Methomyl) was studied, indicating the potential for Ag NPs to degrade halocarbon pesticides through electron transfer processes. The study provides valuable insights into the green synthesis of Ag NPs and their potential applications in various fields, including environmental remediation and agriculture.

Keywords: Ag NPs, Bioreduction, Green synthesis, Halocarbon pesticides, Orange peel extract, Organic pollutants.

Introduction

Nanotechnology is a fascinating and diverse subject matter of research that revolves around manipulating, constructing, and assembling materials with outstanding properties and functions

Published Online First: July, 2024
https://doi.org/10.21123/bsj.2024.9346
P-ISSN: 2078-8665 - E-ISSN: 2411-7986
Baghdad Science Journal

at the nanoscale dimension[1]. This attractive field investigates the world of atoms and molecules, where scientists and researchers use their extensive physics, chemistry, and biology knowledge to design materials with an extraordinary ability to be controlled and precise[2–4]. Nanotechnology has permitted the development of nanomaterials such as nanoparticles and nanocomposites that have distinct properties from their bulk counterparts[5]. Understanding and controlling the size of nanoparticles is crucial, as it directly impacts their physical and chemical properties. Size-dependent phenomena such as surface plasmon resonance[6], catalytic activity[7], and optical properties[8] make nanoparticle size a critical parameter in various fields. These materials have a wide range of applications, including energy storage, catalysis, water purification[9], and drug delivery[10].

Silver nanoparticles are well-known for their catalytic and antibacterial properties due to their distinctive surface chemistry, enabling them to serve as efficient catalysts for various chemical reactions, such as the degradation of organic compounds[11–13]. Additionally, the antibacterial activity of Ag NP makes it safe to use in environmental remediation[14]. The reaction of silver nanoparticles with halogens, such as fluorine (F), chlorine (Cl), bromine (Br), or iodine (I), to produce silver halide compounds represents the mechanism of the dehalogenation of halocarbon compounds. Because of the difference in the electronegativity of halogens and silver (halogens have a higher electronegativity than silver), ionic compounds will form as a result of the reaction between silver and halogens[15,16].

To satisfy the unique requirements of various applications, a variety of methods have been employed to create nanoparticles of various sizes and shapes[17]. Green synthesis is one of the safest and most environmentally friendly techniques because it does not produce any potentially harmful by-products that might negatively impact the environment[18]. The utilization of plant extract as a reductant and stabilizing agent significantly influences the meticulous synthesis of Ag NPs, profoundly affecting the morphology, particle sizes, surface charge, and stability of the metal nanoparticles[19]. Manipulating the physicochemical parameters, including the concentration of silver nitrate, stirring time, and quantity of plant extract employed, allows for deliberate control over these characteristics[20].

Several natural extracts, including those from plants like orange peels, are used as reducing and stabilizing agents during the green synthesis of nanoparticles. Flavonoids, terpenoids, and other organic molecules with functional groups like -COOH (carboxylic acid), -OH (hydroxyl), -C=O (carbonyl), etc. are among the bioactive substances found in these extracts[21–23]. These functional groups may be extremely important for capping or stabilizing the produced nanoparticles as well as for the reduction of metal ions[24]. The release of an electron from the phenolic component is the process by which the interaction of silver ions (Ag^+) with biomolecules is proposed for the reaction to occur. Silver nanoparticles are formed when this electron, which is released after the breakage of the H bond within the -OH group, reduces Ag^+ to Ag^0 [23].

Pesticides are widely used in modern agriculture to protect crops from pests and insects[25]. Pesticides have unique characteristics, such as low biodegradability, high bioaccumulative capacity resulting from their physicochemical features, and a prolonged half-life of 5–15 years, which increases their toxicity to both humans and the environment[26]. Due to the potential for aggravation in the food chain and the development of amounts that are hazardous to human health, the persistent presence of pesticides in surface water, groundwater, soil, and wastewater has become a significant environmental concern[27,28].

The selection of an appropriate water treatment technique (including physical, chemical, and biological methods) for eliminating pesticides depends on both the specific pesticide and the effectiveness of the chosen treatment procedure[26,29]. The photocatalytic degradation of the five most abundant pesticides, including methomyl, by 1% TiO2 or ZnO photocatalysts at a wavelength of 306 nm showed that photolysis of all pesticides was complete under UV radiation for irradiation times between 64 and 100 h[30]. A microwave-induced Fenton-like (FL) hybrid nanoparticle system for the

Published Online First: July, 2024
https://doi.org/10.21123/bsj.2024.9346
P-ISSN: 2078-8665 - E-ISSN: 2411-7986
Baghdad Science Journal

oxidation of methomyl pesticide in wastewater achieved around 91% removal of methomyl after just 8 minutes[31]. Reduced graphene oxide-silver nanocomposite was used to degrade various organohalides, including aliphatic halocarbons and pesticides. The composite exhibited a high adsorption capacity of up to 1534 mg/g [32]. The synthesized NiO-CdO-ZnO mixed ternary oxide nanocomposite, consisting of pure NiO, CdO, and ZnO, showed great potential as a photocatalyst under sunlight[33]. For the photodecomposition of Methylene Blue (MB) dye in wastewater, NiCuMoO/rGO nanocomposite was employed[34]. The catalyst may not be effective in degrading a wide range of contaminants or in different environmental conditions. The degradation of synthetic dyes under solar light was successfully carried out using photocatalysts composite materials[35–38]. Long irradiation times for photocatalytic degradation, generating, and maintaining UV radiation can lead to higher operational costs and environmental concerns related to energy consumption, and nanocomposites can involve complex and costly manufacturing processes that need to prompt more economical and straightforward approaches for the decomposition of organic pollutants. The degradation of halocarbon pesticides can thus be promoted by using metal nanoparticles as a potential method of enhancing the dehalogenation process[32,39,40].

The primary objective of this study was to employ the environmentally friendly green synthesis approach using orange peel extract as a reducing agent to produce Ag NPs. The study sought to comprehensively analyze the structural, optical, and chemical characteristics of the synthesized nanoparticles while also exploring their potential interactions with specific pesticides. The novelty of this study, firstly, is to show the ability of metal nanoparticles to degrade halocarbon pesticides through the dehalogenation process. Secondly, detecting pesticide degradation with FTIR spectroscopy through observation of changes in the structure of halocarbon pesticides (Cypermethrin, Lambda-cyhalothrin) is unlike using harmful cancerous UV light as a light source in photocatalytic degradation. Finally, to increase the study's practicality, we used three pesticides (Cypermethrin, Lambda-cyhalothrin, and Methomyl) that are commonly used by farmers in Kirkuk City. This comprehensive investigation aimed to advance our understanding of the properties and applications of Ag NPs synthesized through this eco-friendly method, contributing to the fields of sustainable nanotechnology and innovative solutions for environmental and agricultural challenges.

Materials and Methods

1. Preparation of Peel Extracts

Fresh orange fruits (Citrus sinensis L. var. baladi) were collected from local markets in Iraq. The fruits were peeled with a sharp knife, washed with distilled water, and then 25 g of orange peels were soaked in 100 ml of deionized water, boiled on a magnetic stirrer for 30 minutes, and then left to cool down. The orange peel solution was filtered with Whatman No1 filter paper and preserved for the second step of synthesizing Ag NPs.

2. Preparation of Silver Nanoparticles

For the green synthesis of silver nanoparticles, 500 ml of three different concentrations of silver nitrate solution (0.5, 1, and 2 moles) were prepared. Then, 30 ml of orange peel extract was added dropwise to each of the three silver nitrate solutions that were prepared and boiled. A change in the colorless silver nitrate solutions into colloidal suspension confirmed the biosynthesis of silver nanoparticles.

3. Pesticides Used in the Study

Three commercially available pesticides in the local market of Kirkuk City were utilized, and 150 µg/ml of prepared Ag NPs were mixed with each of them. These pesticides are Cypermethrin ($C_{22}H_{19}Cl_2NO_3$), Lambda-cyhalothrin ($C_{23}H_{19}ClF_3NO_3$), and Methomyl ($C_5H_{10}N_2O_2S$), denoted as CYP, LC, and M, respectively. In this study, the recommended concentrations of each pesticide have been utilized in agriculture. The graphical representation of fabricated Ag NPs is depicted in Fig. 1.

Published Online First: July, 2024
https://doi.org/10.21123/bsj.2024.9346
P-ISSN: 2078-8665 - E-ISSN: 2411-7986
Baghdad Science Journal

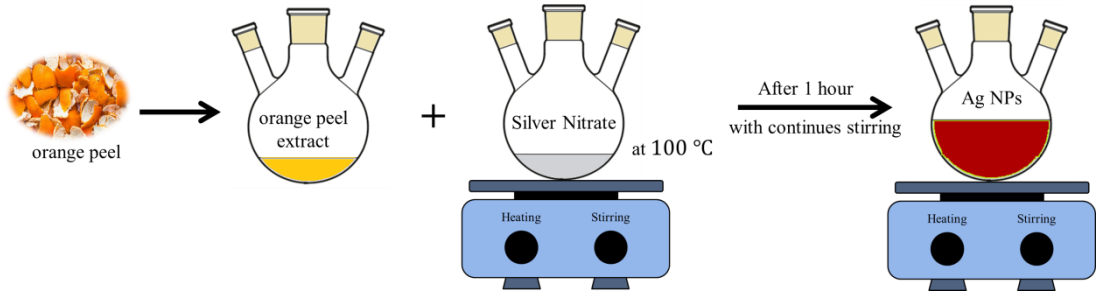

Figure 1. The graphical illustration of fabricated Ag NPs.

4. Characterization

The analysis of the synthesis of Ag-NPs was performed using a T92+ UV Spectrophotometer (PG INSTRUMENTS) (United kingdom) for UV-VIS spectroscopy, which provided critical information on their plasmonic resonance. The UV-VIS spectrophotometer was used to scan the Ag-NPs solution from 350 to 750 nm at 2 nm intervals, utilizing an optical-quality quartz cuvette with a 1 cm path length. The crystalline structures of Ag-NPs were determined using a DX-2700BH Multipurpose X-ray Diffractometer (XRD) (China) with Cu-Ka radiation. The XRD sample of Ag-NPs was prepared by drying the Ag-NPs solution on a glass surface and scanning from 20° to 80°. The size of Ag-NPs was investigated using an EM 208S Transmission Electron Microscope (TEM) (The Netherlands), while their stability was determined using a HORIBA SZ-100 zeta size analyzer (Japan) with an electrode voltage of 3.3 V. To predict the interaction between Ag-NPs and the functional groups present in the chemical compound used, a BROKER ALPHA II Fourier Transform Infrared (FTIR) (Germany) spectrometer was employed. The sample was scanned from a wavenumber of 4000 to 400 cm^{-1}.

Results and Discussion

1. Visual observation of nanoparticles formations

Fig. 2 depicts the production of silver nanoparticles, characterized by a distinct visual confirmation observed through the change in color of the silver nitride solution from a colorless state, as shown in Fig. 2 (a), after the addition of orange peel extract, as indicated by the color shown in Fig. 2 (b). The introduction of orange peel extract into the solution leads to a remarkable transformation, resulting in three different colors, as shown in Figs. 2 (c), (d), and (e). These colors vary depending on the concentration of silver nitride utilized in the process. A key player in this bioreduction process is chlorogenic acid, a primary class of phenolic acids abundantly present in orange peel extract[41]. With its chemical formula $C_{16}H_{18}O_9$, chlorogenic acid serves as an effective reducing agent, facilitating the conversion of silver ions into silver nanoparticles. Its significant presence in the orange peel extract highlights the potential of natural compounds in nanoparticle synthesis, a sustainable approach, and an environmentally friendly method for producing Ag NPs.

Published Online First: July, 2024
https://doi.org/10.21123/bsj.2024.9346
P-ISSN: 2078-8665 - E-ISSN: 2411-7986
Baghdad Science Journal

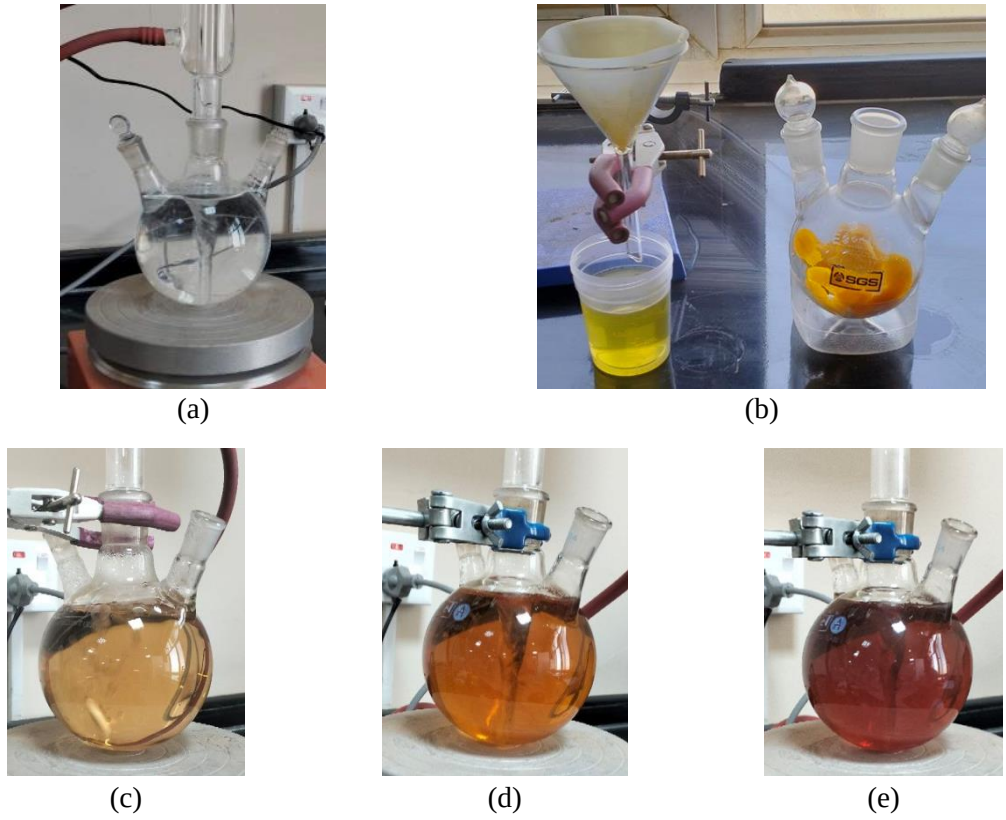

Figure 2. Identifying the formation of nanoparticles through a visual representation of the green synthesis of Ag NPs from (a) orange peel extract and (b) silver nitride solution, (c) 0.5 M, (d) 1M, and (e) 2M silver nitride concentrations.

2. Transmission Electron Microscope (TEM)

The morphology of the grown nanostructures was investigated using TEM, which provided insights into their structural characteristics. The results demonstrated the achievement of Ag NPs with a quasi-spherical shape, thereby confirming the success of the synthesis process, as shown in Fig. 3. In addition to the confirmation of the quasi-spherical morphology, the obtained histogram size distribution provided further quantitative insights into the size variations of the Ag NPs. The histogram revealed average diameters of 20 nm, 30 nm, and 40 nm for the nanoparticles, as illustrated in Figs. 3(a), 2(b), and 2(c), respectively. These distinct average sizes indicated that the concentration of silver nitride employed during the synthesis process played a significant role in influencing the final size of the fabricated nanoparticles. The experimental results clearly indicate a strong correlation between the size of the resulting nanoparticles and the concentration of silver nitride. By altering the concentration of silver nitride, it was possible to control the size of the fabricated Ag NPs. Lower concentrations tended to produce smaller nanoparticles, while higher concentrations yielded larger ones [42]. Increasing the concentration of $AgNO_3$ results in an increase in the amount of silver ions in the solution, which facilitates the growth of NSPs and leads to the development of larger-sized particles [43]. The relevance of this synthesis technique is demonstrated by the successful synthesis of quasi-spherical Ag NPs and the observed dependency on silver nitride concentration for size control[44].

Published Online First: July, 2024
https://doi.org/10.21123/bsj.2024.9346
P-ISSN: 2078-8665 - E-ISSN: 2411-7986
Baghdad Science Journal

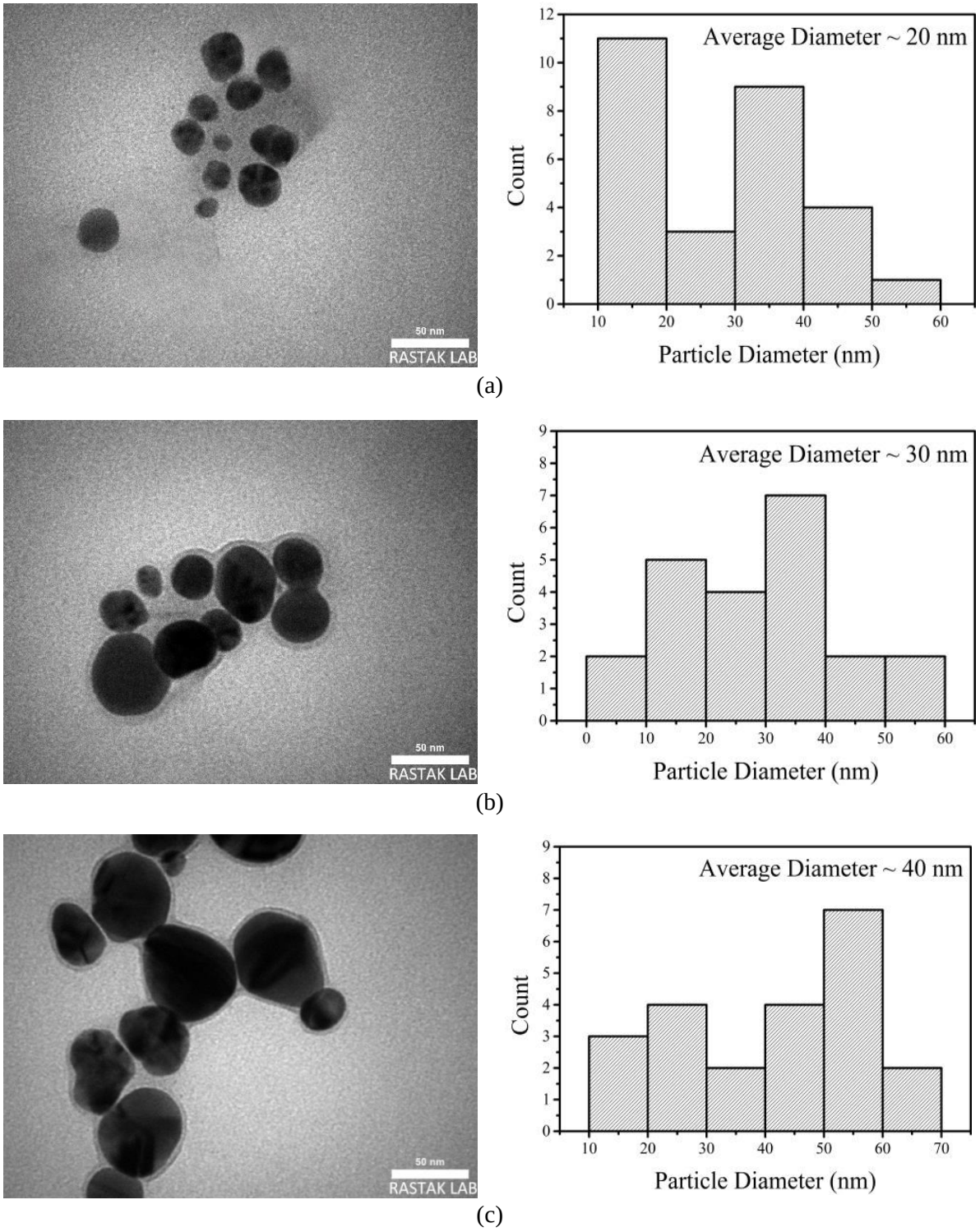

Figure 3. TEM images and associated histograms of (a) 20 nm, (b) 30 nm, and (c) 40 nm Ag NPs

3. Ultraviolet–Visible Spectroscopy (UV-VIS Spectroscopy)

Fig. 4, demonstrates the collection of UV-VIS spectra within the wavelength range of 350–750 nm using a high-quality quartz cuvette with a path length of 1 cm. Through detailed spectral analysis, it was observed that Ag NPs of different sizes exhibited absorption peaks at average wavelengths of 427 nm, 429 nm, and 437 nm for sizes of 20 nm,

Published Online First: July, 2024
https://doi.org/10.21123/bsj.2024.9346
P-ISSN: 2078-8665 - E-ISSN: 2411-7986
Baghdad Science Journal

30 nm, and 40 nm, respectively. Interestingly, as the size of the nanoparticles changed, significant changes occurred in the electronic energy levels present within them. These changes were responsible for a redshift of absorption peaks as the nanoparticle size increased [45], where the absorption peaks shifted towards longer wavelengths[44]. Moreover, this increase in nanoparticle size was also accompanied by the appearance of a broadband absorption peak, indicating a broader range of light absorption tendencies[46]. Broadband absorption is the result of particle-to-particle plasmonic coupling within the cavity among nanoparticles of large sizes[47]. These results show the connection between nanoparticle size and optical characteristics, providing insightful information for further study and practical applications in numerous fields.

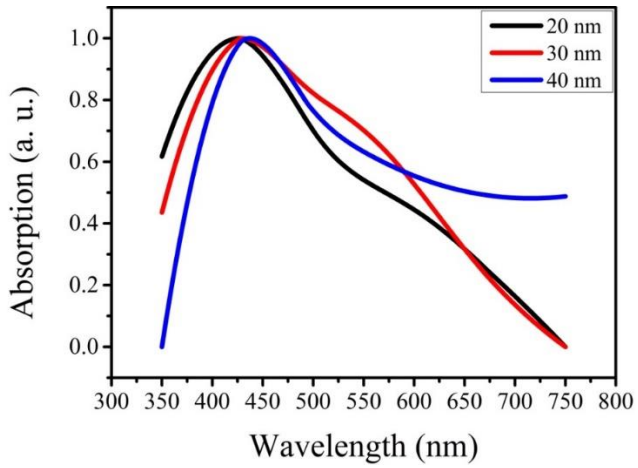

Figure 4. UV-VIS spectra of fabricated nanoparticles

4. Zeta potential analysis

The zeta potential of a nanoparticle is an essential characteristic that describes the electric potential difference between a solid nanoparticle and the surrounding colloidal suspension[48]. It serves as a crucial indicator of the electrostatic attraction or repulsion between nanoparticles present in a dispersion[14]. The magnitude of the electrical charge or potential on the nanoparticles provides valuable insights into the stability of the particles[49]. Generally, nanoparticles exhibit good stability when the zeta potential value exceeds ±30 mV. In contrast, if the zeta potential values fall below ±10 mV, it suggests weak repulsion, which significantly increases the chances of particle instability and aggregation. Nanoparticles with low zeta potential tend to aggregate over time due to the influence of Vander Waal inter-particle interactions, resulting in the formation of larger particle clusters or aggregates. The zeta potential values of -26.6 mV, -25 mV, and -24 mV were observed for fabricated nanoparticles of sizes 20 nm, 30 nm, and 40 nm, respectively. These values indicate a moderate level of stability as they fall within the range of greater than 10 and less than 30, as depicted in Fig. 5 of normalized intensity.

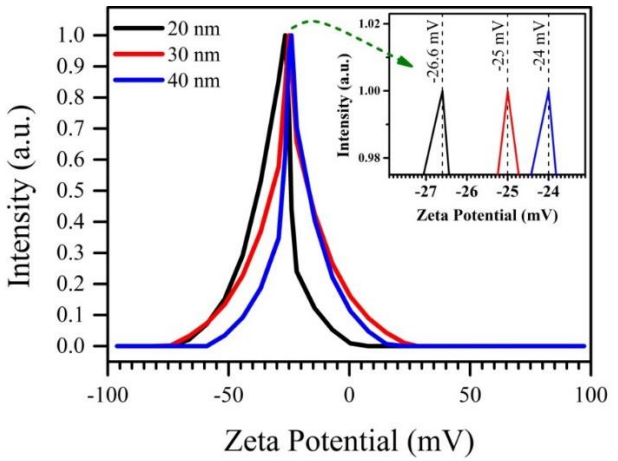

Figure 5. Zeta potential of fabricated nanoparticles

5. XRD analysis

The X-ray diffraction (XRD) technique is a valuable tool for characterizing the crystal planes of thin films and nanostructures that align parallel to the substrate surface. In this context, Fig. 6 illustrates the XRD results obtained for fabricated Ag NPs. It is noteworthy that all the examined samples exhibit a polycrystalline structure. The diffraction pattern reveals distinct peaks corresponding to the (111), (200), (220), and (311) orientations, observed at diffraction angles of 38.1, 44.3, 64.4, and 77.5 degrees, respectively. These findings, characterized by ICDD no. 01-087-0717, provide evidence of a cubic crystal structure for the Ag NPs. Furthermore, the XRD analysis confirms that the samples are single-phase, as only the characteristic diffraction peaks of the face-centered cubic (FCC) phase of Ag are observed. The average measured lattice constant was approximately 4.086Å with an error percentage of 0.008 compared to the value in the above-mentioned ICDD card,

Published Online First: July, 2024
https://doi.org/10.21123/bsj.2024.9346
P-ISSN: 2078-8665 - E-ISSN: 2411-7986
Baghdad Science Journal

adding further validation to the obtained data. Thus, XRD serves as a powerful technique for examining the structural properties of thin films and nanostructures, aiding in their comprehensive characterization and analysis[50].

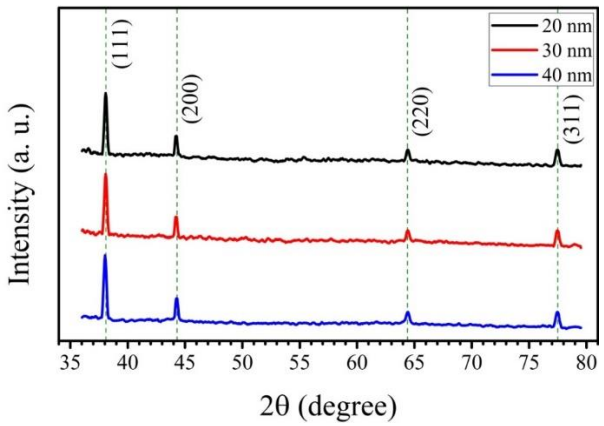

Figure 6. XRD pattern of fabricated nanoparticles

Based on experimental data from X-ray diffraction measurements, the crystallite size was estimated using Eq. 1 (Scherrer equation). The Full Width at Half Maximum (FWHM) of the XRD peak and the crystallite size are related by the Scherrer equation, and from this relationship, the average crystallite size for each nanoparticle sample was calculated.

$$D = 0.9\lambda / \beta \cos\theta \qquad 1$$

D is the crystallite size, λ is the X-ray wavelength, θ is the Bragg angle, and β is full width at half maximum (FWHM).

The average crystallite size for the three sets of Ag NPs with diameters of 20 nm, 30 nm, and 40 nm has been calculated using Eq. 1. The results show that the average crystallite sizes for these samples are approximately 11.0839 nm, 11.0694 nm, and 10.2993 nm, for diameters of 20 nm, 30 nm, and 40 nm, respectively. Table 1 presents the fitting results for all the nanoparticle samples, showing the calculated crystallite sizes along with other relevant parameters.

Table 1. Lattice parameters of fabricated nanoparticles

samples	(hkl)	FWHM (Å)	dhkl (Å)	D (nm)
20 nm Ag NPs	(111)	0.2691	2.3600	15.5065
	(200)	0.2379	2.0431	15.0987
	(220)	0.3134	1.4456	7.8700
	(311)	0.3499	1.2307	5.8606
30 nm Ag NPs	(111)	0.2702	2.3600	15.4465
	(200)	0.2545	2.0431	14.1202
	(220)	0.2907	1.4456	8.4824
	(311)	0.3292	1.2307	6.2286
40 nm Ag NPs	(111)	0.2838	2.3600	14.7256
	(200)	0.2611	2.0431	13.7428
	(220)	0.3689	1.4456	6.6855
	(311)	0.3394	1.2307	6.0431

6. FTIR Analysis

Fig. 7 represents the FTIR spectra of orange peel extract and fabricated Ag NPs, which confirm the functional groups on the nanoparticles' surfaces. The orange peel extract and the green-synthesized Ag NPs FTIR spectra were compared, and all samples' infrared absorption bands were very similar. Orange peel extract showed vibration stretches at 3280 cm^{-1} and 1642 cm^{-1}, corresponding to O-H stretch and C=C stretch, respectively. The results are in good agreement with those found in the literature[18,51]. The peak shifted from 3280 cm^{-1} to 3286 cm^{-1}, 3290 cm^{-1}, and 3292 cm^{-1}, and functional groups at 1648 cm^{-1}, 1642 cm^{-1}, and 1642 cm^{-1} were observed in the FTIR spectra of Ag NPs synthesized by orange peel extract for sizes of 40 nm, 30 nm, and 20 nm, respectively. From the above result, it can be seen that the functional groups in the orange peel extract can bind to the surface of the nanoparticles, producing FTIR

Published Online First: July, 2024
https://doi.org/10.21123/bsj.2024.9346
P-ISSN: 2078-8665 - E-ISSN: 2411-7986
Baghdad Science Journal

spectra that are comparable to those of the extract [23]. The presence of specific functional groups from the orange peel extract on the surface of the synthesized Ag NPs is indicated by the similarity between the FTIR spectra of the Ag NPs and the orange peel extract. These functional groups serve as stabilizers, improving the nanoparticles' stability and bioactivity. The result demonstrates the sustainable nature and environmental friendliness of the green synthesis process[52].

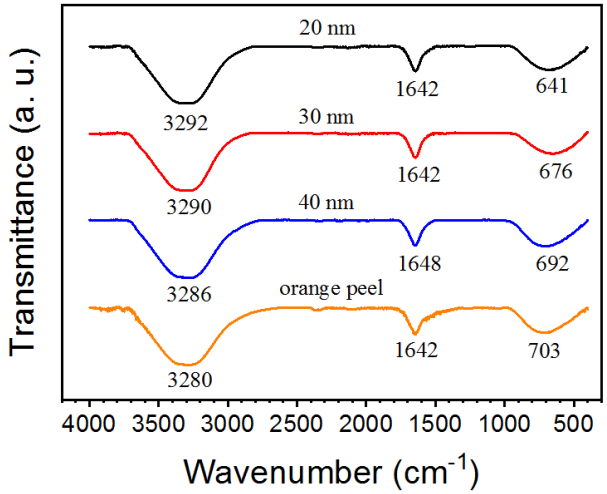

Figure 7. FTIR spectra of orange peel extract and fabricated Ag NPs

The functional groups of the three commercially available pesticides on the local market were investigated and depicted in Fig. 8. (Cypermethrin, Lambda-cyhalothrin, and Methomyl, which were denoted as CYP, LC, and M, respectively). For CYP, the following functional groups were observed at 3294 cm^{-1}, 1642 cm^{-1}, 1401 cm^{-1}, and 658 cm^{-1}, which correspond to O-H stretch, C=C stretch, O-H bending, and C-Cl stretching, respectively [53]. For LC, the functional groups were observed at 3341 cm^{-1}, 1642 cm^{-1}, 1062 cm^{-1}, and 695 cm^{-1}, corresponding to O-H stretch, C=C stretch, O-H bending, and C-Cl stretching, respectively [54]. For M, the functional groups were observed at 3324 cm^{-1}, 1642 cm^{-1}, and 670 cm^{-1}, which correspond to O-H stretch, C=C stretch, and C=C bending, respectively [55].

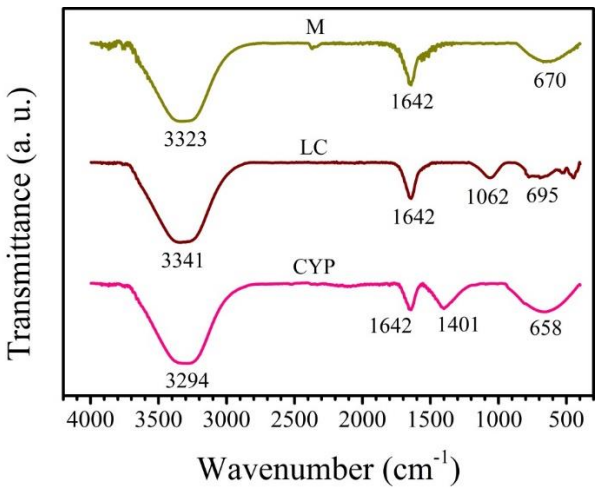

Figure 8. FTIR spectra of the pesticides Cypermethrin (CYP), Lambda-cyhalothrin (LC), and Methomyl (M).

7. Interaction of Ag NPs with Pesticides

FTIR spectra analysis was conducted to study the interactions of three different sizes of Ag NPs (40 nm, 30 nm, and 20 nm) with three specific pesticides, namely Cypermethrin, Lambda-cyhalothrin, and Methomyl, as shown in Fig. 9, Fig. 10, and Fig. 11, respectively. Fig. 9 and Fig. 10 illustrate the changes in transmittance within the FTIR spectra due to the presence of Ag NPs in the pesticide environment. A notable decrease in transmittance at wavenumbers 1401 cm^{-1} and 1062 cm^{-1} indicates a significant alteration in the molecular structure of both Cypermethrin and Lambda-cyhalothrin pesticides. Such reductions in peak intensities are indicative of chemical changes and the occurrence of degradation processes. These results show that metal nanoparticles assist in the dehalogenation process, resulting in the degradation of halocarbon pesticides[32,39,40]. The following processes are involved in the potential mechanism for the degradation of halocarbon pesticide compounds in the presence of noble metal nanoparticles: The surface of noble metal nanoparticles is first adsorbed with halocarbon pesticide molecules. The noble metal nanoparticles then assist electron transfer processes with the halocarbon pesticide molecules that have been adsorbed on their surface. This electron transfer weakens the pesticide molecule's carbon-halogen bond. Finally, the weaker carbon-halogen bond exposes the halocarbon pesticide to nucleophilic

Published Online First: July, 2024
https://doi.org/10.21123/bsj.2024.9346
P-ISSN: 2078-8665 - E-ISSN: 2411-7986
Baghdad Science Journal

attack from nearby water molecules. Water behaves as a nucleophile, donating a pair of electrons to the carbon atom, causing the carbon-halogen bond to breakdown[56–58]. The decrease in absorption peaks in Fig. 9 and Fig. 10 is more pronounced when the size of nanoparticles is reduced. This phenomenon is attributed to the nanoparticles' increased surface area, which facilitates higher adsorption of pesticide molecules onto the surface of Ag NPs. Fig. 11 shows that there are no significant alterations in transmittance, which can be attributed to Methomyl not being categorized as a halocarbon pesticide. As a result, the absence of halocarbon properties in Methomyl hinders the degradation of non-halocarbon pesticides by Ag NPs. Numerous studies have proposed that the photodegradation of Methomyl using semiconductor nanoparticles proves to be an efficient approach for its degradation[30,59,60].

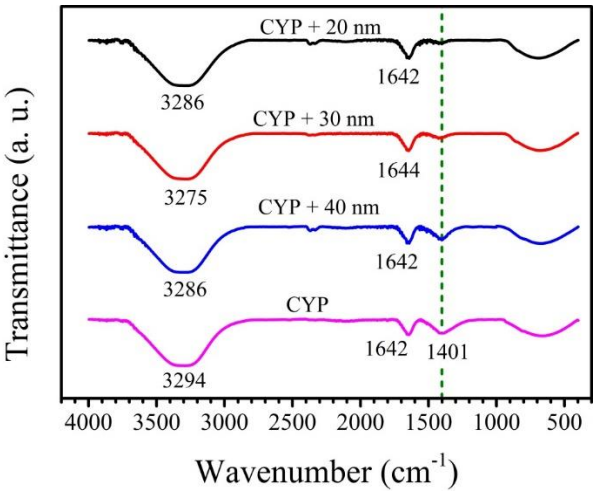

Figure 9. FTIR spectra of the interaction between Ag NPs and the Cypermethrin (CYP) pesticide.

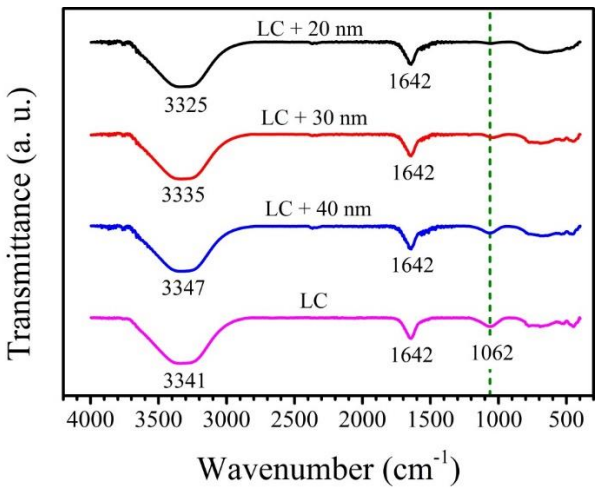

Figure 10. FTIR spectra of the interaction between Ag NPs and the Lambda-cyhalothrin (LC) pesticide.

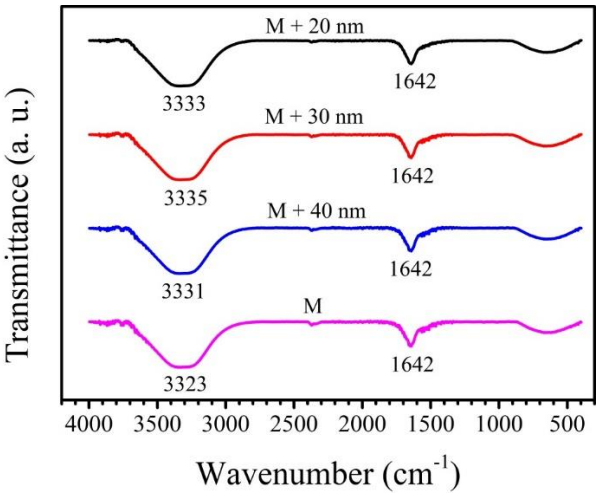

Figure 11. FTIR spectra of the interaction between Ag NPs and the Methomyl (M) pesticide.

Conclusion

The successful green fabrication of silver nanoparticles (Ag NPs) utilizing orange peel extract as a reducing agent is demonstrated in this study. The formation of Ag NPs with different colors corresponding to different sizes 20 nm, 30 nm, and 40 nm was confirmed visually by varying the concentration of silver nitride (0.5, 1, and 2 moles). TEM analysis revealed quasi-spherical Ag NPs, and their size was found to depend on the concentration of silver nitride during fabrication. UV-VIS spectroscopy provided insights into the nanoparticles' optical properties, with absorption peak redshifts observed as nanoparticle size increased (427 nm, 429 nm, and 437 nm for 20 nm, 30 nm, and 40 nm sizes, respectively). Zeta potential measurements indicated modest stability for the synthesized nanoparticles, with values of -26.6 mV, -25 mV, and -24 mV for 20 nm, 30 nm, and 40 nm nanoparticles, respectively. XRD analysis confirmed the cubic crystal structure of Ag

Published Online First: July, 2024
https://doi.org/10.21123/bsj.2024.9346
P-ISSN: 2078-8665 - E-ISSN: 2411-7986
Baghdad Science Journal

NPs, with crystallite sizes of approximately 11.0839 nm, 11.0694 nm, and 10.2993 nm for 20 nm, 30 nm, and 40 nm nanoparticles, respectively. FTIR analysis revealed the presence of functional groups from the orange peel extract on the Ag NPs' surface, contributing to their bioactivity and stability. The interaction of Ag NPs with halocarbon pesticides, Cypermethrin and Lambda-Cyhalothrin, led to significant changes in their molecular structures due to the breakdown process promoted by the noble metal nanoparticles. However, no substantial alterations were observed with the non-halocarbon pesticide, Methomyl. The study illustrates the potential of green synthesis utilizing natural substances and its impact on the properties of Ag NPs. The results provide valuable insights for prospective uses in environmental remediation and agriculture. The eco-friendly method contributes to the growing interest in green nanotechnology for nanoparticle synthesis.

Acknowledgment

The authors gratefully acknowledge the Department of Chemistry and Environmental Research Unit, College of Science, University of Kirkuk, Iraq, for their assistance.

Authors' Declaration

- Conflicts of Interest: None.
- We hereby confirm that all the Figures and Tables in the manuscript are ours. Furthermore, any Figures and images, that are not ours, have been included with the necessary permission for re-publication, which is attached to the manuscript.
- No animal studies are present in the manuscript.
- No human studies are present in the manuscript.
- Ethical Clearance: The project was approved by the local ethical committee in University of Kirkuk.

Authors' Contribution Statement

The proposed idea was conceived by R. B. A. The data was acquired by H. R. R. The analysis was carried out by H. R. R, H. B. A, and R. B. A. The data were interpreted by H. B. A and R. B. A. The paper's drafter is H. R. R. The article was revised and proofread by H. B. A and R. B. A. All authors read the manuscript carefully and approve the final version of their MS.

References

1. Loza K, Heggen M, Epple M. Synthesis, Structure, Properties, and Applications of Bimetallic Nanoparticles of Noble Metals. Adv Funct Mater. 2020; 30(21): 1909260(1of14). https://doi.org/10.1002/adfm.201909260
2. Liang J, Liu Q, Li T, Luo Y, Lu S, Shi X, et al. Magnetron Sputtering Enabled Sustainable Synthesis of Nanomaterials for Energy Electrocatalysis. Green Chem. 2021; 23(8): 2834–2867. https://doi.org/10.1039/D0GC03994B
3. Abdulrahman HB, Krajczewski J, Kudelski A. Modification of Surfaces of Silver Nanoparticles for Controlled Deposition of Silicon, Manganese, and Titanium Dioxides. Appl Surf Sci. 2018; 427: 334–339. https://doi.org/10.1016/j.apsusc.2017.08.163
4. Samuel MS, Ravikumar M, John J. A, Selvarajan E, Patel H, Chander PS, et al. A Review on Green Synthesis of Nanoparticles and Their Diverse Biomedical and Environmental Applications. Catalysts. 2022; 12(5): 459(1of24). https://doi.org/10.3390/catal12050459
5. Shareef HA, Jafar NB, Abdulrahman RB. The Biosynthesis of Silver Nanoparticles by Moringa Oleifera and its Antibacterial Activity. Indian J Public Heal Res Dev. 2019; 10(8): 2052-2057. https://doi.org/10.5958/0976-5506.2019.02157.0
6. Kiba T, Masui K, Inomata Y, Furumoto A, Kawamura M, Abe Y, et al. Control of Localized Surface Plasmon Resonance of Ag Nanoparticles by Changing its Size and Morphology. Vacuum. 2021; 192: 110432(1of7). https://doi.org/10.1016/j.vacuum.2021.110432
7. Saim AK, Adu PCO, Amankwah RK, Oppong MN, Darteh FK, Mamudu AW. Review of Catalytic Activities of Biosynthesized Metallic Nanoparticles in Wastewater Treatment. Environ Technol Rev.

Published Online First: July, 2024
https://doi.org/10.21123/bsj.2024.9346
P-ISSN: 2078-8665 - E-ISSN: 2411-7986
Baghdad Science Journal

2021; 10(1): 111–130. https://doi.org/10.1080/21622515.2021.1893831
8. Salih AI. Color Characterizations of Pure ZnO and ZnO/ SeO2 Thin Films Annealed at Different Temperature. Kirkuk J Sci. 2021; 15(4): 107–124. https://doi.org/10.32894/kujss.2021.167522
9. Zhao J, Shao Q, Ge S, Zhang J, Lin J, Cao D, et al. Advances in Template Prepared Nano Oxides and their Applications: Polluted Water Treatment, Energy, Sensing and Biomedical Drug Delivery. Chem Rec. 2020; 20(7): 710–729. https://doi.org/10.1002/tcr.201900093
10. Haidary SM, Mohammed AB, Córcoles EP, Ali NK, Ahmad MR. Effect of Coatings and Surface Modification on Porous Silicon Nanoparticles for Delivery of the Anticancer Drug Tamoxifen. Microelectron Eng. 2016; 161: 1–6. https://doi.org/10.1016/j.mee.2016.03.051
11. Rabeea MA, Owaid MN, Muslim RF. Synthesis and characterization of silver nanoparticles by natural organic compounds extracted from Eucalyptus leaves and their role in the catalytic degradation of methylene blue dye. Songklanakarin J Sci Technol. 2021; 43(1): 14–23. https://doi.org/10.14456/sjst-psu.2021.3
12. David L, Moldovan B. Green Synthesis of Biogenic Silver Nanoparticles for Efficient Catalytic Removal of Harmful Organic Dyes. Nanomaterials. 2020; 10(2): 202. https://doi.org/10.3390/nano10020202
13. Zakaria MA, Menazea AA, Mostafa AM, Al-Ashkar EA. Ultra-thin silver nanoparticles film prepared via pulsed laser deposition: Synthesis, characterization, and its catalytic activity on reduction of 4-nitrophenol. Surf Interfaces. 2020; 19: 100438. https://doi.org/10.1016/j.surfin.2020.100438
14. Abbas AZ, Abdulrahman RB, Mustafa TA. Preparation and Characterization of Silver Nanoparticles and its Medical Application against Pathogenic Bacteria. Baghdad Sci J. 2023. https://doi.org/10.21123/bsj.2023.7763
15. Nair AS, Pradeep T. Halocarbon mineralization and catalytic destruction by metal nanoparticles. Curr. Sci. 2003;84(12): 1560–1564. http://www.jstor.org/stable/24108263
16. Nair AS, Tom RT, Suryanarayanan V, Pradeep T. ZrO2 bubbles from core–shell nanoparticles. J Mater Chem. 2003; 13(2): 297–300. https://doi.org/10.1039/b210734a
17. Alsumaidaei FKT, Mohammed HA. The Effect of Addition of (Al2O3) Nano Particles on Structural and Electrical Properties of Bi2Ba2Ca2Cu3O10" +δ" Superconductors at High Temperature. Kirkuk J Sci. 2020; 15(4): 1–18. https://doi.org/10.32894/kujss.2020.167506
18. Niluxsshun MCD, Masilamani K, Mathiventhan U. Green Synthesis of Silver Nanoparticles from the Extracts of Fruit Peel of Citrus tangerina, Citrus sinensis, and Citrus limon for Antibacterial Activities. Bioinorg. Chem Appl. 2021; 2021: 1–8. https://doi.org/10.1155/2021/6695734
19. Jadoun S, Arif R, Jangid NK, Meena RK. Green Synthesis of Nanoparticles Using Plant Extracts: A review. Environ Chem Lett. 2021; 19(1): 355–374. https://doi.org/10.1007/s10311-020-01074-x
20. Wan Mat Khalir WKA, Shameli K, Jazayeri SD, Othman NA, Che Jusoh NW, Hassan NM. Biosynthesized Silver Nanoparticles by Aqueous Stem Extract of Entada spiralis and Screening of Their Biomedical Activity. Front Chem. 2020; 8: 1–15. https://doi.org/10.3389/fchem.2020.00620
21. Viñas-Ospino A, Panić M, Bagović M, Radošević K, Esteve MJ, Radojčić Redovniković I. Green Approach to Extract Bioactive Compounds From Orange Peel Employing Hydrophilic and Hydrophobic Deep Eutectic Solvents. Sustain. Chem Pharm. 2023; 31: 100942. https://doi.org/10.1016/j.scp.2022.100942
22. Saini RK, Ranjit A, Sharma K, Prasad P, Shang X, Gowda KGM, et al. Bioactive Compounds of Citrus Fruits: A Review of Composition and Health Benefits of Carotenoids, Flavonoids, Limonoids, and Terpenes. Antioxidants. 2022; 11(2): 239(1of27). https://doi.org/10.3390/antiox11020239
23. Mogole L, Omwoyo W, Viljoen E, Moloto M. Green synthesis of silver nanoparticles using aqueous extract of Citrus sinensis peels and evaluation of their antibacterial efficacy. Green Process Synth. 2021; 10(1): 851–859. https://doi.org/10.1515/gps-2021-0061
24. Alsharari SS, Alenezi MA, Al Tami MS, Soliman M. Recent advances in the Biosynthesis of Zirconium Oxide Nanoparticles and their Biological Applications. Baghdad Sci J. 2023; 20(1): 41-57. https://doi.org/10.21123/bsj.2022.7055
25. Abdul Latif M, Al-Salhi A, Kata Y, Muhammad M. The Role of the Agricultural Extension in Educating Farmers about the Legislation on Protecting the Environment from Pollution with Chemical Pesticides. Kirkuk Univ J Agric Sci. 2023; 14(1): 218–229. https://doi.org/10.58928/ku23.14118
26. Saleh IA, Zouari N, Al-Ghouti MA. Removal of Pesticides From Water and Wastewater: Chemical, Physical and Biological Treatment Approaches. Environ Technol Innov. 2020; 19: 101026. https://doi.org/10.1016/j.eti.2020.101026
27. Bruckmann FS, Schnorr C, Oviedo LR, Knani S, Silva LFO, Silva WL, et al. Adsorption and Photocatalytic Degradation of Pesticides into Nanocomposites: A Review. Molecules. 2022; 27(19): 6261(1of27). https://doi.org/10.3390/molecules27196261
28. Pebdeni AB, Khurshid CA, Abkenar SD, Hosseini M. Green Synthesis of Carbon Quantum Dots Doped on Nickel Oxide Nanoparticles as Recyclable Visible Light Photocatalysts for Enhanced Degradation of Malachite Green. ChemistrySelect.

Published Online First: July, 2024
https://doi.org/10.21123/bsj.2024.9346
P-ISSN: 2078-8665 - E-ISSN: 2411-7986
Baghdad Science Journal

2021; 6(20): 5034–5042. https://doi.org/10.1002/slct.202101116
29. Kalaf FI, Mustafa TA, Haidar Hassan AA. Use Some Nanomaterials as Insecticides Against the Saw-Toothed Grain Beetle Oryzaephilus Surinamensis L. (Coleoptera: Silvanidae). Kirkuk Univ J Agric Sci. 2022; 13(3): 159–174. https://doi.org/10.58928/ku22.13313
30. EL-Saeid MH, BaQais A, Alshabanat M. Study of the Photocatalytic Degradation of Highly Abundant Pesticides in Agricultural Soils. Molecules. 2022; 27(3): 634(1of13). https://doi.org/10.3390/molecules27030634
31. Tony MA, Mansour SA. Microwave Assisted Catalytic Oxidation of Methomyl Pesticide by Cu/Cu2O/CuO Hybrid Nanoparticles as a Fenton-like Source. Int J Environ Sci Technol. 2020; 17(1): 161–174. https://doi.org/10.1007/s13762-019-02436-x
32. Koushik D, Sen Gupta S, Maliyekkal SM, Pradeep T. Rapid Dehalogenation of Pesticides and Organics atthe Interface of Reduced Graphene Oxide–Silver Nanocomposite. J Hazard Mater. 2016; 308: 192–198. https://doi.org/10.1016/j.jhazmat.2016.01.004
33. Munawar T, Iqbal F, Yasmeen S, Mahmood K, Hussain A. Multi metal oxide NiO-CdO-ZnO nanocomposite–synthesis, structural, optical, electrical properties and enhanced sunlight driven photocatalytic activity. Ceram Int. 2020; 46(2): 2421–2437. https://doi.org/10.1016/j.ceramint.2019.09.236
34. Areej F, Munawar T, Mukhtar F, Nadeem MS, Akbar UA, Hakeem AS, et al. Synthesis and characterization of rGO-supported Mo/Cu dual-doped NiO nanocomposite for the elimination of dye pollutant. Appl Nanosci. 2023; 13(8): 5641–5657. https://doi.org/10.1007/s13204-023-02786-6
35. Nadeem MS, Munawar T, Mukhtar F, Rabbani AW, ur Rehman N, Mahmood K, et al. Facile synthesis of PANI and rGO supported Y/Pr co-doped ZnO: boosted solar light-driven photocatalysis. Appl Phys A. 2023; 129(6): 450(1of9). https://doi.org/10.1007/s00339-023-06701-2
36. Sardar S, Munawar T, Mukhtar F, Nadeem MS, Khan SA, Koc M, et al. Fullerene trigged energy storage and photocatalytic ability of La2O3-ZnO@C60 core-shell nanocomposite. Mater Sci Eng B. 2023; 288: 116151. https://doi.org/10.1016/j.mseb.2022.116151
37. Oliveira TP, Rodrigues SF, Marques GN, Viana Costa RC, Garçone Lopes CG, Aranas C, et al. Synthesis, Characterization, and Photocatalytic Investigation of CuFe2O4 for the Degradation of Dyes under Visible Light. Catalysts. 2022; 12(6): 623. https://doi.org/10.3390/catal12060623
38. Nadeem MS, Munawar T, Mukhtar F, Rabbani AW, Khan SA, Koc M, et al. Synergistic photocatalytic properties of fullerene (C60) anchored V/Cu dual-doped NiO nanocomposites for water disinfection. Mater Sci Eng B. 2023; 297(6): 116705(1of12). https://doi.org/10.1016/j.mseb.2023.116705
39. Vigneshwaran S, Sirajudheen P, Karthikeyan P, Nabeena CP, Meenakshi S. Remediation of Persistent Organic Pesticides from Wastewater Matrices - Present and Future Conceptions. Pollution Control Technologies Energy, Environment, and Sustainability. 2021: 7–37. https://doi.org/10.1007/978-981-16-0858-2
40. Handojo L, Ikhsan NA, Mukti RR, Indarto A. Agrochemicals Detection, Treatment and Remediation. Chap 20: Nanomaterials for remediations of agrochemicals. Elsevier; 2020: 535–567. https://doi.org/10.1016/B978-0-08-103017-2.00020-9
41. Mostafa YS, Alamri SA, Alrumman SA, Hashem M, Baka ZA. Green Synthesis of Silver Nanoparticles Using Pomegranate and Orange Peel Extracts and Their Antifungal Activity against Alternaria solani, the Causal Agent of Early Blight Disease of Tomato. Plants. 2021; 10(11): 2363(1of18). https://doi.org/10.3390/plants10112363
42. Sharifi Dehsari H, Halda Ribeiro A, Ersöz B, Tremel W, Jakob G, Asadi K. Effect of precursor concentration on size evolution of iron oxide nanoparticles. Cryst Eng Comm. 2017; 19(44): 6694–6702. https://doi.org/10.1039/C7CE01406F
43. Ahmad N, Ang BC, Amalina M A, Bong CW. Influence of Precursor Concentration and Temperature on the Formation of Nanosilver in Chemical Reduction Method. Sains Malaysiana. 2018; 47(1): 157–168. https://doi.org/10.17576/jsm-2018-4701-19
44. Hussein RA, Ibrahim MN, Abdulrahman RB. Histological And Physiological Assessment Of Silver Nanoparticles (AgNPs) On The Kidneys Of Albino Mice. J Pharm Negat Results. 2022; 13(Special Issue7): 685–696. https://doi.org/https://doi.org/10.47750/pnr.2022.13.S07.92
45. Abdulrahman RB, Alagoz AS, Karabacak T. Enhanced Light Trapping in Periodic Aluminum Nanorod Arrays as Cavity Resonator. MRS Proc. Cambridge University Press; 2013; 1566(1): mrss13-1566-ii09-06. https://doi.org/10.1557/opl.2013.878
46. Li H, Hu Y, Yang Y, Zhu Y. Theoretical Investigation of Broadband Absorption Enhancement in a-Si Thin Film Solar Cell with Nanoparticles. Sol Energy Mater Sol Cells. 2020; 211: 110529(1of6). https://doi.org/10.1016/j.solmat.2020.110529
47. Abdulrahman RB, Cansizoglu H, Cansizoglu MF, Herzog JB, Karabacak T. Enhanced light trapping and plasmonic properties of aluminum nanorods fabricated by glancing angle deposition. J Vac Sci Technol A. American Vacuum Society; 2015;33(4): 41501. https://doi.org/10.1116/1.4919737

Published Online First: July, 2024
https://doi.org/10.21123/bsj.2024.9346
P-ISSN: 2078-8665 - E-ISSN: 2411-7986
Baghdad Science Journal

48. Serrano-Lotina A, Portela R, Baeza P, Alcolea-Rodriguez V, Villarroel M, Ávila P. Zeta potential as a tool for functional materials development. Catal Today. 2023; 423: 113862(1of11). https://doi.org/10.1016/j.cattod.2022.08.004
49. Doghish AS, Hashem AH, Shehabeldine AM, Sallam A-AM, El-Sayyad GS, Salem SS. Nanocomposite based on gold nanoparticles and carboxymethyl cellulose: Synthesis, characterization, antimicrobial, and anticancer activities. J Drug Deliv Sci. Technol. 2022; 77: 103874(1of20). https://doi.org/10.1016/j.jddst.2022.103874
50. Majeed Khan MA, Kumar S, Ahamed M, Alrokayan SA, AlSalhi MS. Structural and Thermal Studies of Silver Nanoparticles and Electrical Transport Study of Their Thin Films. Nanoscale Res Lett. 2011; 6(1): 434(1of8). https://doi.org/10.1186/1556-276X-6-434
51. Alzahrani E. Colorimetric Detection Based on Localized Surface Plasmon Resonance Optical Characteristics for Sensing of Mercury Using Green-Synthesized Silver Nanoparticles. J Anal Methods Chem. 2020; 2020: 1–14. https://doi.org/10.1155/2020/6026312
52. Sreelekha E, George B, Shyam A, Sajina N, Mathew B. A Comparative Study on the Synthesis, Characterization, and Antioxidant Activity of Green and Chemically Synthesized Silver Nanoparticles. Bionanoscience. 2021;11(2): 489–496. https://doi.org/10.1007/s12668-021-00824-7
53. Altug DT, Kinayturk NK, Tunali B. The use of pumice to prevent penetration of cypermethrin into the soil. Fresenius Environ. Bull. 2020; 29(12 A): 11266–11272.
54. Kumar TT, Jahangir HS. Bio-degradation of lambda-cyhalothrin by Rhodococcus erythropolis. life science informatics . 2018; 4(5): 192-208. https://doi.org/10.26479/2018.0405.15
55. Nurhalisa DA, Andayani S, La Ode Baytul Abidin VN. Insecticide With Active Methomyl Ingredients Against Hematological Parameters As Information on Stress Conditions of Tilapia Strain Jatimbulan (Oreochromis niloticus). J Surv Fish Sci. 2023; 10(3S): 3462–3477. https://doi.org/10.17762/sfs.v10i3S.1198
56. Bootharaju MS, Pradeep T. Understanding the Degradation Pathway of the Pesticide, Chlorpyrifos by Noble Metal Nanoparticles. Langmuir. 2012; 28(5): 2671–2679. https://doi.org/https://doi.org/10.1021/la2050515
57. Yin H, Cao X, Lei C, Chen W, Huang B. Insights into Electroreductive Dehalogenation Mechanisms of Chlorinated Environmental Pollutants. Chem Electro Chem. 2020; 7(8): 1825–1837. https://doi.org/10.1002/celc.202000067
58. Nair AS, Tom RT, Kumar VRR, Subramaniam C, Pradeep T. Chemical Interactions at Noble Metal Nanoparticle Surfaces — Catalysis, Sensors and Devices. COSMOS. 2007; 03(01): 103–124. https://doi.org/10.1142/S0219607707000244
59. Tony MA, Purcell PJ, Mansour SA. Photodegradation and Box-Behnken Design Optimization for Methomyl Using Fenton Process Based on Synthesized CuO Nanocrystals Via Facile Wet Chemical Technique. Chem Eng Commun. 2021; 208(3): 349–363. https://doi.org/10.1080/00986445.2020.1719079
60. Luna-Sanguino G, Ruíz-Delgado A, Tolosana-Moranchel A, Pascual L, Malato S, Bahamonde A, et al. Solar Photocatalytic Degradation of Pesticides Over TiO2-rGO Nanocomposites at Pilot Plant Scale. Sci Total Environ. 2020; 737: 140286(1of27). https://doi.org/10.1016/j.scitotenv.2020.140286

Published Online First: July, 2024
https://doi.org/10.21123/bsj.2024.9346
P-ISSN: 2078-8665 - E-ISSN: 2411-7986
Baghdad Science Journal

توصيف التصنيع الأخضر لجسيمات الفضة النانوية باستخدام مستخلص قشر البرتقال وتأثيرها على تحلل المركبات الكيميائية الهالوكربونية

هشام رشيد رحمان[1]، هيمن برهان الدين عبدالرحمن[2]، روژه برهان الدين عبدالرحمن [1]

[1]قسم الفيزياء، كلية العلوم، جامعة كركوك، كركوك، العراق.
[2]فرع الادوية والسموم، كلية الصيدلة، جامعة كركوك، كركوك، العراق.

الخلاصة

ان دور النانوتكنولوجيا في معالجة الملوثات العضوية يعتبر ذو أهمية كبيرة، نظراً للتأثيرات الجوهرية على البيئة التي تنشأ عن الاستخدام الواسع للمبيدات الحشرية في الزراعة. وبالتالي، تم تسليط الضوء بشكل خاص على المواد النانوية الامتصاصية بسبب خصائصها الاستثنائية وقدرتها على تحلل وإزالة ملوثات عضوية متعددة بفعالية، بما في ذلك المبيدات الحشرية. في هذه الدراسة، تم العمل على تصنيع وتوصيف جسيمات الفضة النانوية باستخدام مستخلص قشر البرتقال كعامل مختزل حيوي. اثبتت صور TEM على تكون الشكل الشبه الكروي لجسيمات الفضة النانوية ، حيث تصل أحجامها المتوسطة الى 40 نانومتر و 30 نانومتر و 20 نانومتر وفقاً لتراكيز نترايت الفضة المختلفة (2 و1 و 0.5 مول) ، على التوالي . كما أظهرت تحليل UV-VIS تواجد ذروات امتصاص عند الطول موجي 427 نانومتر و 429 نانومتر و 437 نانومتر لأحجام الجسيمات 20 نانومتر و 30 نانومتر و 40 نانومتر، على التوالي، مما يسلط الضوء على العلاقة بين الحجم والخصائص البصرية للجسيمات النانوية. أظهر تحليل جهد زيتا استقراراً معتدلاً للجسيمات المصنوعة، ذات قيم 26.6- ملي فولت و 25- ملي فولت و 24- ملي فولت للجسيمات ذات الاحجام 20 نانومتر و 30 نانومتر و 40 نانومتر، على التوالي. وأكدت تحليل XRD على تكون بنية متعددة البلورات ذات الطور المكعبي لجسيمات الفضة النانوية وبأحجام بلورية تبلغ حوالي 11.0839 نانومتر و11.0694 نانومتر و10.2993 نانومتر للجسيمات النانوية 20 نانومتر و30 نانومتر و40 نانومتر على التوالي. وأوضح تحليل FTIR على وجود مجموعات وظيفية من مستخلص قشر البرتقال على سطوح الجسيمات النانوية، الذي يعزز فعاليتها البيولوجية بالأضافة الى دورها في استقرار جسيمات الفضة النانوية. تمت دراسة التفاعل بين جسيمات الفضة النانوية وثلاث مبيدات حشرية مختلفة (سيبرميثرين، لامبدا-سايالوثرين، وميثوميل)، واشارت النتائج إلى إمكانية تحلل المبيدات الهالوكربونية بواسطة جسيمات الفضة النانوية عن طريق عمليات نقل الإلكترونات. تقدم هذه الدراسة رؤى قيمة حول التخليق الأخضر لجسيمات الفضة النانوية واستخداماتها المحتملة في مجموعة متنوعة من المجالات، مثل تحسين البيئة والزراعة.

الكلمات المفتاحية: Ag NPs، الاختزال الحيوي، التخليق الأخضر مبيدات الهالوكربون، مستخلص قشر البرتقال، الملوثات العضوية.